

COMPARISON OF HRDI WIND MEASUREMENTS WITH RADAR AND ROCKET OBSERVATIONS

M.D. Burrage,<sup>1</sup> W.R. Skinner,<sup>1</sup> A.R. Marshall,<sup>1</sup> P.B. Hays,<sup>1</sup> R.S. Lieberman,<sup>1</sup> S.J. Franke,<sup>2</sup>  
 D.A. Gell,<sup>1</sup> D.A. Ortland,<sup>1</sup> Y.T. Morton,<sup>1</sup> F.J. Schmidlin,<sup>3</sup> R.A. Vincent,<sup>4</sup> and D.L. Wu<sup>1</sup>

**Abstract.** Wind fields in the mesosphere and lower thermosphere are obtained with the High Resolution Doppler Imager (HRDI) on the Upper Atmosphere Research Satellite (UARS) by observing the Doppler shifts of emission lines in the O<sub>2</sub> Atmospheric band. The validity of the measured winds depends on an accurate knowledge of the positions on the detector of the observed lines in the absence of a wind induced Doppler shift. These positions have been determined to an accuracy of approximately 5 ms<sup>-1</sup> from the comparison of winds measured by HRDI with those obtained by MF radars. Excellent agreement is found between HRDI measured winds and winds observed with radars and rockets. In addition, the sensitivity of HRDI to migrating tides and other large scale waves is demonstrated.

1. Introduction

The High Resolution Doppler Imager (HRDI) on the Upper Atmosphere Research Satellite (UARS) is designed to measure horizontal winds in the mesosphere and lower thermosphere and in the stratosphere. One of the objectives of the HRDI investigations is to develop a comprehensive global climatology of the winds in the altitude range 65-105 km. This will serve as a reference point for future studies and provide comparison for global models. To date, most studies of this region have employed the view of the circulation based on COSPAR International Reference Atmosphere (CIRA) data obtained from meteorological rockets prior to 1970. More recent wind observations carried out with a network of radars show features not present in the CIRA climatology [e.g. Balsley and Riddle, 1984; Tetenbaum et al., 1986; Manson et al., 1987]. This report outlines the procedure by which systematic errors in the HRDI data are inferred, and demonstrates the consistency of HRDI wind measurements with other observational techniques and the applicability of HRDI observations to studies of large scale mesospheric waves.

HRDI is a triple etalon Fabry-Perot Interferometer [Hays et al., 1993], which is used to observe the very small wind induced Doppler shifts of absorption and emission rotational lines in the O<sub>2</sub> Atmospheric ( $b^1\Sigma_g^+ - X^3\Sigma_g^-$ ) bands [Abreu et al., 1989]. In the mesosphere and lower thermosphere, 'A' (0 - 0) band emission features are observed, the brightness and self-absorption of which are dependent on the rotational line quantum number J. Lower J valued lines are typically brighter but suffer from more self-absorption, and the choice of which line to use depends on altitude. As the atmosphere is penetrated more deeply, a balance must be struck between line brightness and self-absorption. Therefore, in order to scan the atmosphere from 65 to 105 km, rotational lines of three different strengths are used. The scan is performed in both an upward and a downward direction at approximately the same geographical location. Measurements collected during the downward scan at lower altitudes (65 - 85 km) employ a line of weaker intensity that is not significantly

self-absorbed, while a stronger line is used at higher altitudes (85 - 105 km). For the upward scan, a line of 'medium strength' is used at all altitudes. The wavenumbers and the relative line strengths observed with the operational mode most commonly used for the mesosphere and lower thermosphere, which employs two different viewing azimuths, are indicated in Table 1. The use of two lines at each altitude allows the temperature and volume emission rate to be determined from the ratio of the line strengths. Because of the large change in the spacecraft velocity and Earth rotation component of the Doppler shift between the two azimuths, it was not possible for the weak intensity case to find a single line that fell within the detector range for both viewing directions.

The HRDI instrument incorporates a fully gimbaled telescope, which collects light from the atmosphere and allows limb scans to be performed at any azimuth. Vector winds are determined by observing the same atmospheric volume from two nearly orthogonal viewing directions. This is achieved by employing the pointing capability of the telescope and the spacecraft motion. Usually, the telescope observes a region of the atmosphere in a direction or azimuth angle of 45° to the spacecraft velocity vector, and 9 minutes later nearly the same atmospheric volume is sampled by using a telescope azimuth of 135°. On a given day, observations are carried out on only one side of the spacecraft, either the warm (sun) side or the cold side, and this determines the latitudinal coverage of the data. The Doppler shift measured by the instrument is a weighted average of the velocity component at each altitude along the line of sight (LOS). Profiles of the LOS velocity must be mathematically inverted using the known weighting functions to obtain the actual wind. The inversion of HRDI data is carried out using a sequential estimation technique based on the method of Rodgers [1976; 1990]. An effect of the inversion process is that real vertical and horizontal variations may be smoothed, while any systematic error in the LOS measurement will be distorted.

The LOS wind is derived from the measured centroid position,  $v_m$ , of an absorption or emission line on the detector, and is given by

$$v = v_m - v_0(v, \phi) - \alpha(T - T_0) - f(t) - v_s \cos \epsilon \cos \theta - \frac{2\pi R_E}{T_E} \sin \psi \cos \theta \quad (1)$$

where all of the terms in Eq. (1) have velocity units. The term  $v_0$  corresponds to the zero wind reference position, which is a function of the wavenumber,  $\nu$ , and the azimuth of the observation,  $\phi$ . The parameter  $\alpha$  denotes the sensitivity of the line position to the mean temperature of the instrument,  $T$ , relative to a reference temperature,  $T_0$ . The long term drift of the instrument arising from the gradual adjustment to the space environment (outgassing) is represented by a function of time,  $f(t)$ . The terms  $\alpha$  and  $f(t)$  are obtained using observations of spectral lines of onboard calibration lamps. These calibrations are carried out every day, and the derived temperature and long term drift corrections are accurate to within a few ms<sup>-1</sup> (Skinner et al., Atmospheric Wind Measurements with The High Resolution Doppler Imager (HRDI), 1993). The final two terms of Eq. (1) are corrections which must be applied to account for the spacecraft velocity,  $v_s$ , and the Earth rotation, where  $\epsilon$  is the elevation angle of the observation,  $R_E$  and  $T_E$  are the radius and rotation period of the Earth, and  $\theta$  and  $\psi$  are the latitude and observation bearing angle from north.

An accurate knowledge of the component of the spacecraft velocity and the Earth rotation in the viewing

<sup>1</sup>Space Physics Research Laboratory, University of Michigan,

<sup>2</sup>Department of Electrical and Computer Engineering, University of Illinois

<sup>3</sup>Goddard Space Flight Center, Wallops Flight Facility

<sup>4</sup>Department of Physics and Math Physics, University of Adelaide

Copyright 1993 by the American Geophysical Union.

Paper number 93GL01108

0094-8534/93/93GL-01108\$03.00

TABLE 1. Wavenumbers and relative strengths of emission lines employed by the HRDI mesosphere and lower thermosphere scanning mode.

Alt. (km)	Azimuth 45°		Azimuth 135°	
	Up scan	Down scan	Up scan	Down scan
65-85	13076.318 (medium)	13052.316 (weak)	13076.318 (medium)	13041.118 (weak)
85-105	13076.318 (medium)	13138.194 (strong)	13076.318 (medium)	13138.194 (strong)

direction is essential. The spacecraft velocity is about 7500  $\text{ms}^{-1}$ , so even a small uncompensated component will seriously affect the wind determination. The uncertainty in the required correction lies not in the accuracy of the satellite velocity, which is known to better than 1  $\text{ms}^{-1}$ , but in the location of the telescope viewing direction relative to the satellite trajectory. The spacecraft attitude is known to about 0.01°, which translates to a wind measurement error of only ~1  $\text{ms}^{-1}$ . However, the relationship between the spacecraft reference frame and the telescope frame exhibits a variation which depends mainly on long term changes in the solar heating of the spacecraft. The misalignment between the spacecraft frame and the HRDI instrument frame is measured periodically by observing stars of known position, and yields a correction to the measured winds of the order of 5  $\text{ms}^{-1}$ .

## 2. Zero Wind Position

Because of the large Doppler shifts induced by the spacecraft, which has the effect of moving the spectrum around on the detector, and because of slight non-uniformities in the detector response, it was not practical to try to locate the zero wind reference position,  $v_0$ , during pre-launch calibration. Instead, it is determined using atmospheric wind data collected in orbit in conjunction with dynamical assumptions, and employing correlative measurements made by rockets and radars. The zero wind position depends only on wavelength and telescope azimuth, and was determined to a first order of accuracy using a two step procedure which employs dynamical assumptions. The first step assumes that the global mean winds sampled at about the same local time do not change rapidly over a period of a day or two. By alternating the observations from the warm side (azimuths -45° and -135°) to the cold side (azimuths 45° and 135°) for two consecutive days, it is possible to obtain information on the zero references for the different azimuths since the components of the wind in the 45° and -135° (or -45° and 135°) directions should be of approximately equal magnitude but opposite sign. This geometry is illustrated in Figure 1. The forward viewing line position measurements  $F_{\text{WARM}}$  and  $F_{\text{COLD}}$ , which are corrected for the temporal and thermal drifts and spacecraft and Earth rotation velocities, incorporate the same zero reference position,  $v_{F0}$ , while the backward measurements  $B_{\text{WARM}}$  and  $B_{\text{COLD}}$  each include the reference value,  $v_{B0}$ . If the components of the wind at azimuths -45° and 135° are  $U_{-45}$  and  $U_{135}$ , respectively, then

$$F_{\text{WARM}} = U_{-45} - v_{F0} \quad (2)$$

and

$$B_{\text{COLD}} = U_{135} - v_{B0} \quad (3)$$

If the wind field does not change significantly during the two days taken to collect the warm side and cold side measurements, and the data is averaged over each day for a given latitude, then  $\overline{U_{-45}} = -\overline{U_{135}}$ , and thus

$$\overline{F_{\text{WARM}}} + \overline{B_{\text{COLD}}} = -(v_{F0} + v_{B0}) \quad (4)$$

The determination of the absolute values of  $v_{F0}$  and  $v_{B0}$  requires a second step which uses the assumption that the long-term mean meridional winds are zero. This method employs data sampled symmetrically about the equator in order to remove tidal effects and averaged over a long period to reduce seasonal variations. Since the recovery of any component of the wind requires both viewing directions, the second stage of the procedure also yields an expression involving both  $v_{F0}$  and  $v_{B0}$ . However, they may be separated by substituting for either one of them using the information obtained from the first step [Eq. (4)]. This procedure yields

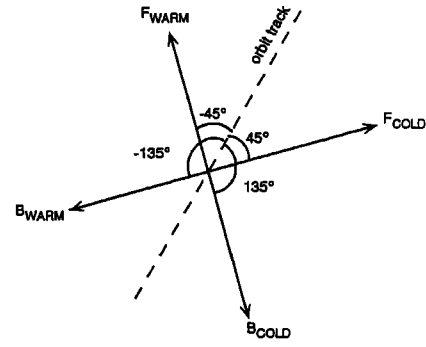


Fig. 1. Schematic diagram illustrating the geometry of HRDI observations made on both the warm and the cold sides of the spacecraft. The measurements  $F_{\text{WARM}}$  and  $F_{\text{COLD}}$  are obtained in the forward directions relative to the satellite trajectory at azimuths of 45° and -45°, and the measurements  $B_{\text{WARM}}$  and  $B_{\text{COLD}}$  are obtained in the backward directions at azimuths of 135° and -135°.

estimates of the zero reference positions obtained from HRDI atmospheric data accurate to within about 10  $\text{ms}^{-1}$ .

## 3. Comparisons Of Wind Observations

Further improvement in the accuracy of the zero reference positions requires the comparison of HRDI measurements with ground based instruments (lidars, radars, etc.), special *in situ* measurements (balloons, rockets), and the results of models and climatology. The problems encountered in comparing satellite remote sensing observations with other types of data have been discussed by Gille et al. [1984]. Correlative instruments generally provide vertical profiles more or less directly above the station, yielding essentially point measurements. In contrast, limb viewing satellite instruments such as HRDI give profiles which are a weighted average along the line of sight. Another difficulty is that the coincidence of the HRDI and correlative measurement is never exact, either in space or time. There are also uncertainties associated with the averaging procedures employed by the different measurement techniques. For example, MF radars may indicate variations in the wind field due to insufficient sampling of short period gravity waves [e.g. Lloyd et al., 1990]. By contrast, HRDI has an effective horizontal resolution of a few hundred km, and therefore does not readily detect such waves. Consequently, a series of consecutive radar wind measurements collected with the typical 5 minute integration period may exhibit significant variability, as is illustrated in Figure 2 by a set of observations made with the Urbana MF radar. The closest HRDI profile, which was obtained approximately 100 km from the radar, is also included in the figure. In order to provide a better comparison with HRDI, an attempt is made to remove the effect of small horizontal structures in the radar data by averaging over a time period of usually 1-2 hours. Because of the different effective spatial and temporal resolutions of the HRDI and correlative measurements and the high degree of short term atmospheric variability, the two techniques are not really sampling the same quantity. In addition, most observational methods (including HRDI) employ filtering techniques which are designed to remove the effects of measurement noise. It is possible that high frequency components that are actually present in the wind profile may be removed as well.

Any differences between HRDI data and other measurements resulting from the problems described above would be random, and therefore statistical comparisons should reveal the systematic errors. One approach is to determine the mean differences between the HRDI and correlative measurements and the standard deviation of the mean differences for each site using as many coincidences as possible (typically 10-50). Wind comparisons are carried out by first transforming the correlative zonal and meridional measurement components to the corresponding HRDI viewing direction. Consistent offsets between the wind observed by HRDI and that obtained using other measurement techniques have already indicated errors in the initial determination of the HRDI zero reference positions. Quantifying the errors from this kind of comparison is

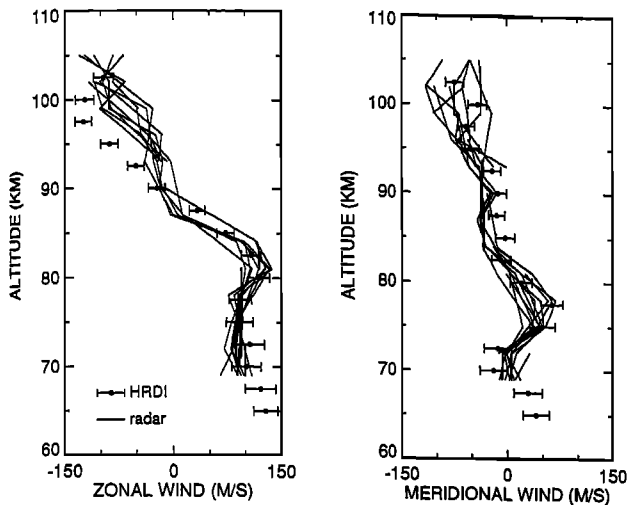


Fig. 2. Series of 5 minute integration wind profiles obtained by the Urbana MF radar between 16:13 and 17:13 UT on December 25, 1991. The HRDI wind measurements, which were made 113 km from the radar site at 16:43 UT, are included for comparison.

difficult since the offset is incorporated into the line of sight measurements, which are then inverted using the sequential estimation technique to yield the wind profile. The inversion process tends to distort systematic errors in the LOS measurements. In addition, the various emission lines which contribute to the final HRDI wind product may have different offset errors. An examination of the LOS wind profile as a function of wavelength is necessary to isolate and quantify the different effects. Line position offset errors determined in this way are used to correct the HRDI database. To date, the zero reference positions of all of the lines listed in Table 1 have been adjusted to obtain the best agreement between HRDI and MF radars located at Urbana (40.2° N, 271.8° E) (Franke and Thorsen, Mean winds and tides in the upper middle atmosphere at Urbana (40° N, 88° W) during 1991-1992, submitted to *J. Geophys. Res.*, 1993), Christmas Island (2.0° N, 202.6° E) [Vincent and Lesicar, 1991] and Adelaide (34.6° S, 138.5° E) [Vincent and Fritts, 1987].

The agreement of the mean winds observed by HRDI and by the Urbana MF radar after adjusting the zero reference values is illustrated in Figure 3 for both the forward and the backward HRDI viewing directions. The figure indicates the mean differences in the wind measurement made by the two techniques and the error bars denote standard deviations of the mean differences. The results were obtained using approximately 40 coincidences with the Urbana radar which occurred between December, 1991 and December, 1992. The radar data was averaged over periods of two hours, centered on the time of the closest approach of the HRDI observation tangent point to the radar station. The maximum spatial displacement of the two measurements was 500 km, and since the effective horizontal resolution of HRDI is of the same magnitude, in the averaging process coincidences were not weighted according to the separation distance but only to the HRDI measurement variance. Figure 3 indicates that the differences between the two techniques vary about zero for both viewing directions, and do not exceed  $5 \text{ ms}^{-1}$  at any altitude.

Comparisons with correlative data sets also provide valuable information on the level of constraint which should be employed by the sequential estimator used to invert the HRDI observations. This parameter controls the degree of horizontal smoothing of the recovered wind profile. An example of a comparison between HRDI winds generated using two different levels of smoothing with those obtained by a rocket is presented in Figure 4. For the HRDI results in Figure 4(a), the sequential estimator employed a relatively weak constraint which effectively averages horizontal structures of scale size less than 500 km. The large vertical variations apparent in the HRDI winds are not supported by the rocket data. Figure 4(b) demonstrates the effect of using a stronger constraint, equivalent to removing structures of scale size less than 1000 km. The amplitude of the vertical

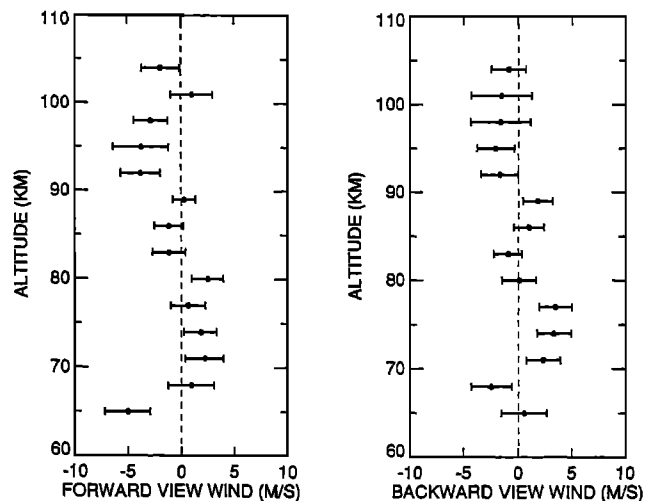


Fig. 3. Mean differences between HRDI and Urbana MF radar winds resolved into (a) the HRDI forward viewing direction (azimuth 45°) and (b) the backward viewing direction (azimuth 135°). The error bars denote standard deviations of the means.

oscillations is much smaller than that for the weaker constraint of the previous figure, greatly improving the agreement with the rocket observations. This suggests that much of the vertical structure in the HRDI winds of Figure 4(a) is due to measurement noise.

The determination of the zero reference positions and the appropriate degree of smoothing to apply to the HRDI wind measurements has yielded results which are in very good agreement with rockets and with MF radars. Figure 5 shows a comparison of the meridional wind profiles measured by HRDI and by the Urbana radar on 12 consecutive days. For each of the profiles, the HRDI measurement was carried out within 300 km of the radar site. The local time of each coincidence varied by about 20 minutes per day, due to the precession of the UARS orbit, and all of the observations presented in Figure 5 were obtained for the local time range 10:30-13:30. Clearly, the two techniques resolve the same vertical structures, and in general these appear to be tidal in nature. In particular, the winds observed on December 20 exhibit a vertical wavelength of ~25 km, consistent with the (1,1) diurnal tide, and there is some suggestion of a downward progression of the oscillation on subsequent days. Obviously other phenomena, such as the semidiurnal tide, non-migrating tides and planetary waves, must also be contributing to the observed winds, particularly on the earlier days shown in the figure. For example, the shorter vertical wavelength of 10-15 km seen on December 15 and 16 is perhaps suggestive of a non-migrating tidal component. When this study is extended to the global view of the wind field provided by HRDI and incorporates measurements from networks of radars and other localized techniques, it should be possible to assess the different contributions of the various dynamical components.

#### 4. Conclusion

The validity of HRDI measured winds relies on an accurate knowledge of the zero wind positions, the effects of thermal and temporal drifts and the LOS component of the spacecraft velocity and Earth rotation. The instrumental drifts are quantified by monitoring the stability of onboard calibration lines, and the spacecraft velocity and Earth rotation corrections are determined by measuring the instrument/spacecraft misalignments using HRDI observations of stars. The absolute values of the reference positions are estimated by applying appropriate dynamical constraints to mean HRDI atmospheric observations. Increased confidence in the HRDI wind retrievals is gained by employing comparisons with correlative measurements. This activity serves not only to establish the validity of the HRDI measurements, but also provides a common baseline which can be used to inter compare the many ground-based observational techniques. In addition, the unique spatial and

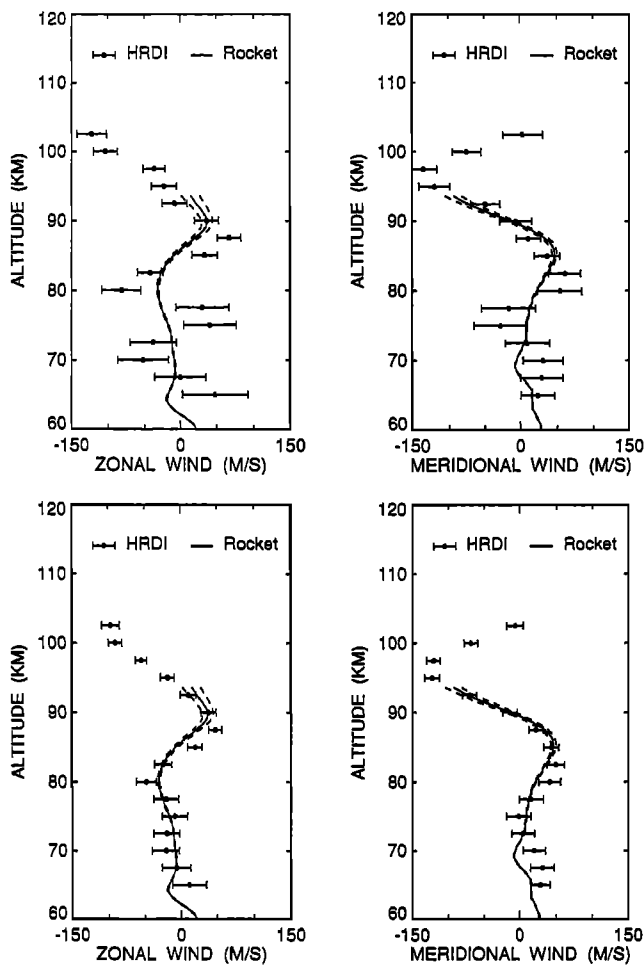


Fig. 4. Wind profiles determined using HRDI at 16:09 UT and a rocket launched from Wallops Island at 16:14 UT on March 25, 1992. The spatial separation between the two sets of measurements was about 300 km, and the solar zenith angle was  $40^\circ$ . The HRDI winds were generated by inverting the line of sight observations with the sequential estimator employing a constraint which effectively averages horizontal structures of (a) scale size less than 500 km, and (b) scale size less than 1000 km.

temporal coverage of the HRDI data base will facilitate the first effective observational test of the accuracy of global dynamical models. Also, great progress will be made with studies of mesospheric dynamics by means of a synthesis of HRDI observations and localized (ground based and *in situ*) measurements. HRDI measurements are fixed in local time for a given day, but have complete longitude coverage which provides important information on non-migrating tides and planetary waves, while localized techniques are fixed in longitude, but cover a range of local times giving a better view of the migrating components.

**Acknowledgments:** This work is sponsored by NASA through Contract No. NAS 5-27751.

#### REFERENCES

Abreu, V. J., A. Bucholtz, A., P. B. Hays, D. A. Ortland, W. R. Skinner, and J. -H. Yee, Absorption and Emission Line Shapes in the  $O_2$  Atmospheric Bands: Theoretical Model and Limb Viewing Simulations, *Appl. Opt.* 28, 2128-2137, 1989.

Balsley, B. B., and A. C. Riddle, Monthly mean values of the mesospheric wind over Poker Flat, Alaska, *J. Atmos. Sci.*, 41, 2368-2375, 1984.

Gille, J. C., J. M. Russell III, P. L. Bailey, L. L. Gordley, E. E. Remsburg, J. H. Lienesch, W. G. Planet, F. B. House, L. V. Lyjak, and S. A. Beck, Validation of temperature retrievals obtained by the Limb Infrared Monitor of the Stratosphere (LIMS) Experiment on NIMBUS 7, *J. Geophys. Res.*, 89, 5147-5160, 1984.

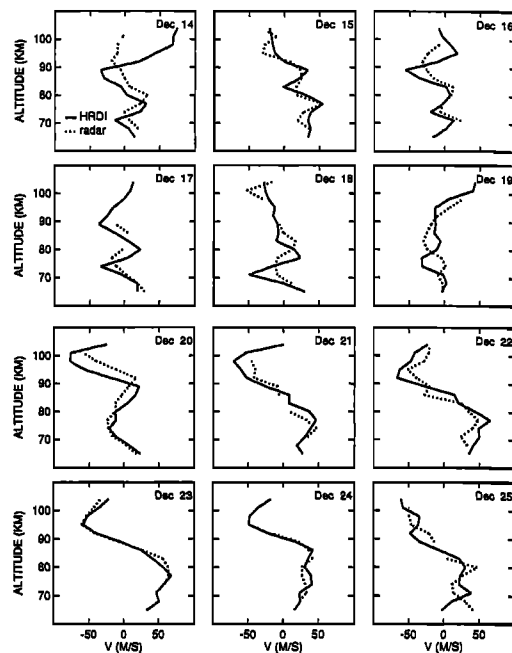


Fig. 5. Comparison of meridional (V) wind profiles measured by HRDI (solid lines) and the Urbana MF radar (broken lines) on 12 consecutive days from December 14 to December 25, 1992.

Hays, P. B., V. J. Abreu, M. E. Dobbs, D. A. Gell, H. J. Grassl, and W. R. Skinner, The High Resolution Doppler Imager on the Upper Atmosphere Research Satellite, *J. Geophys. Res.*, in press, 1993.

Lloyd, N., A. H. Manson, D. J. McEwen, and C. E. Meek, A comparison of middle atmospheric dynamics at Saskatoon ( $52^\circ N$ ,  $107^\circ W$ ) as measured by a medium frequency radar and a Fabry-Perot interferometer, *J. Geophys. Res.*, 95, 7653-7660, 1990.

Manson, A. H., C. E. Meek, M. Massebeuf, J. L. Fellous, W. G. Elford, R. A. Vincent, R. L. Craig, R. G. Roper, S. Avery, B. B. Balsley, G. J. Fraser, M. J. Smith, R. R. Clark, S. Kato, and T. Tsuda, Mean winds of the upper middle atmosphere ( $\sim 70$ -100 km) from the global radar network: comparisons with CIRA 72, and new rocket and satellite data, *Adv. Space Res.*, 7, 143-153, 1987.

Rodgers, C. D., Retrieval of atmospheric temperature and composition from remote measurements of thermal radiation, *Rev. Geophys. and Space Phys.*, 14, 609-624, 1976.

Rodgers, C. D., Characterization and error analysis of profiles retrieved from remote sounding measurements, *J. Geophys. Res.*, 95, 5587-5595, 1990.

Tetenbaum, D., S. K. Avery, and A. C. Riddle, Observations of mean winds and tides in the upper mesosphere during 1980 - 1984, using the Poker Flat, Alaska MST radar as a meteor radar. *J. Geophys. Res.*, 91, 14,539-14,556, 1986.

Vincent, R. A., and D. C. Fritts, A climatology of gravity wave motions in the mesosphere at Adelaide, Australia, *J. Atmos. Sci.*, 44, 748-760, 1987.

Vincent, R. A., and D. Lesicar, Dynamics of the equatorial mesosphere: First results with a new generation partial reflection radar, *Geophys. Res. Lett.*, 18, 825-828, 1991.

M.D. Burrage, D.A. Gell, P.B. Hays, R.S. Lieberman, A.R. Marshall, Y.T. Morton, D.A. Ortland, W.R. Skinner, and D.L. Wu, Space Physics Research Laboratory, University of Michigan, Ann Arbor, MI 48109-2143.

S.J. Franke, Dept. of ECE, University of Illinois, Urbana, IL 61801.

F.J. Schmidlin, Goddard Space Flight Center, Wallops Flight Facility, Wallops Island, VA 23337.

R.A. Vincent, Dept. of Physics and Math Physics, University of Adelaide, Adelaide 5001, Australia.

(Received February 1, 1993;  
revised April 16, 1993;  
accepted April 20, 1993.)